Electronic Supplementary Information
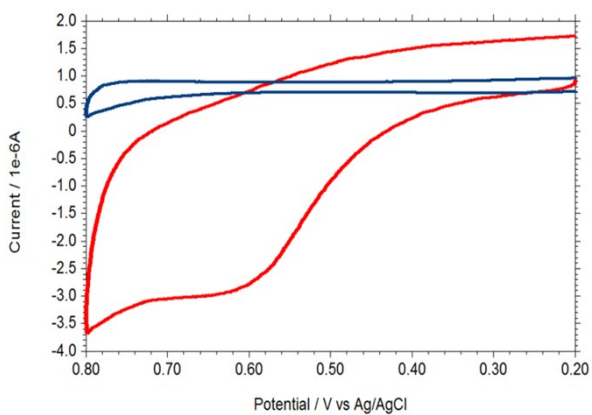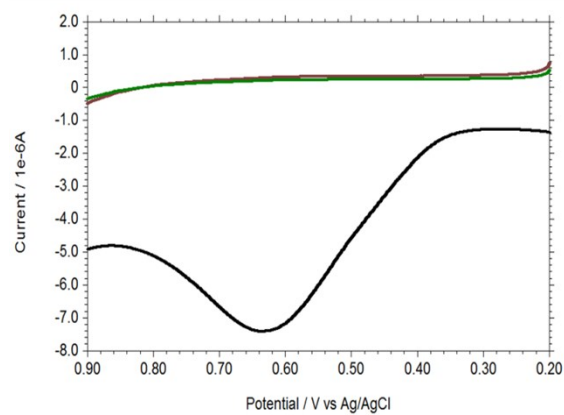
Non-enzymatic electrochemical sensing of glucose and hydrogen peroxide using bis(acetylacetonato)oxovanadium(IV) complex modified gold electrode

Koushik Barman and Sk Jasimuddin[*]

Department of Chemistry, Assam University, Silchar, Assam -788011, India


S1   S2

Figure S1. Overlaid cyclic voltammogram obtained with (red curve) and without (blue curve) 0.1 mM glucose at the [VO(acac)$_2$]-PATP-Au electrode in 0.1 M PBS solution (pH = 7.0).

Figure S2. Overlaid DPV obtained with bare (brown curve), PATP (green curve) and [VO(acac)$_2$]-PATP (black curve) modified gold electrode in 0.1 mM glucose in 0.1 M PBS solution (pH = 7.0).
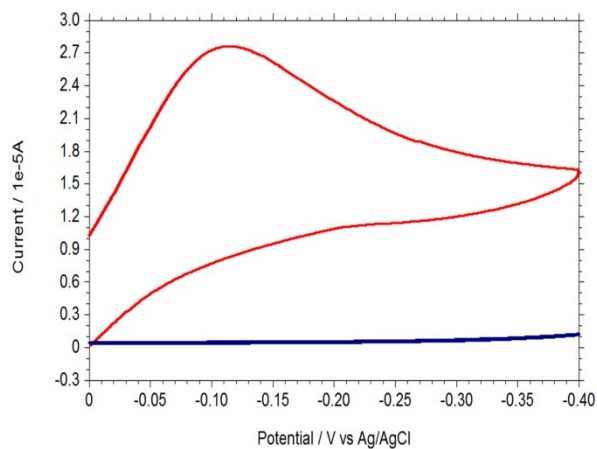

Figure S3. Overlaid cyclic voltammogram obtained with (red curve) and without (blue curve) 0.5 mM H$_2$O$_2$ at the [VO(acac)$_2$]-PATP-Au electrode in 0.1 M PBS solution (pH = 7.0).
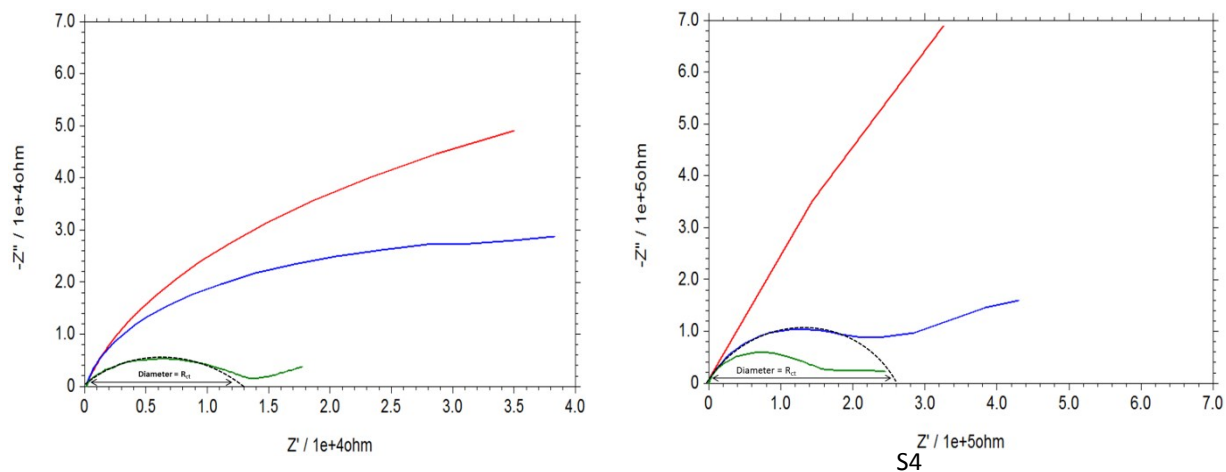
Figure S4. Overlaid Nyquist plot of 0.1 mM glucose in 0.1 M phosphate buffer solution (pH = 7.0) using bare and modified gold electrodes. E_{ac} = 10 mV, frequency range: 0.01-100000 Hz. [bare Au (blue curve), R_{CT} = 4.0 × 10^4 Ω; PATP - Au (red curve), R_{CT} = 4.8 × 10^4 Ω; [VO(acac)$_2$]-PATP-Au (green curve, R_{CT} = 1.3 × 10^4 Ω].

Figure S5. Overlaid Nyquist plot of 0.5 mM H_2O_2 in 0.1 M phosphate buffer solution (pH = 7.0) using bare and modified gold electrodes. E_{ac} = 10 mV, frequency range: 0.01-100000 Hz. [bare Au (blue curve), R_{CT} = 2.6 × 10^5 Ω; PATP-Au (red curve), R_{CT} = 6.4 × 10^5 Ω; [VO(acac)$_2$]-PATP-Au (green curve), R_{CT} = 1.2 × 10^5 Ω]

S6

S7
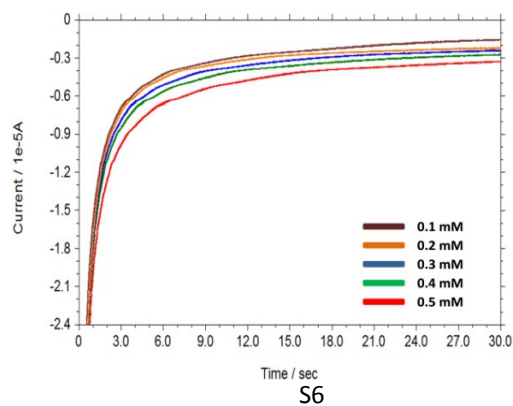
Figure S6. Chronoamperograms with increasing concentration of glucose (0.1 to 0.5 mM) in 0.1 M PBS (pH 7.0) at [VO(aca)2]-4-PATP-Au electrode at + 0.65 V *vs* Ag/AgCl. LOD= 0.1 μM.
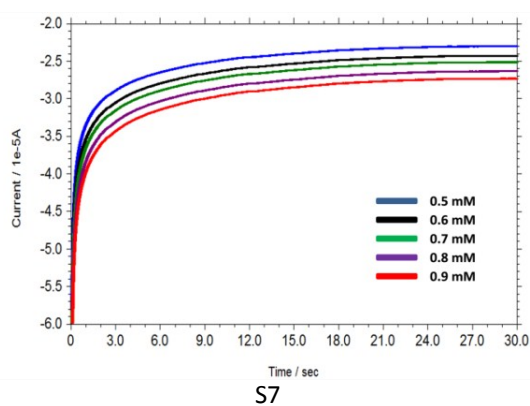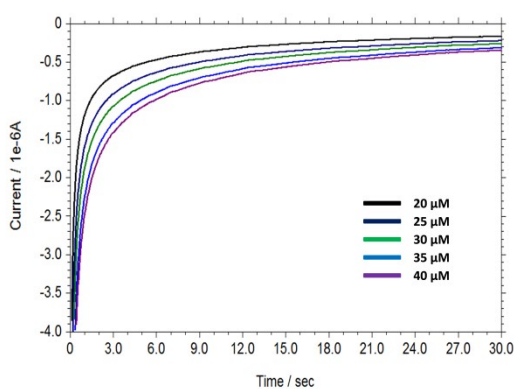
Figure S7. Chronoamperograms with increasing concentration of H_2O_2 (0.5 to 0.9 mM) in 0.1 M PBS (pH 7.0) at [VO(acac)$_2$]-4-PATP-Au electrode at - 0.11 V *versus* Ag/AgCl. LOD = 0.03 μM.
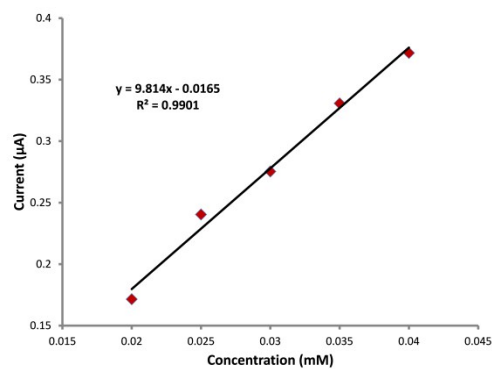

y = 3.725x + 0.0103
R^2 = 0.9969
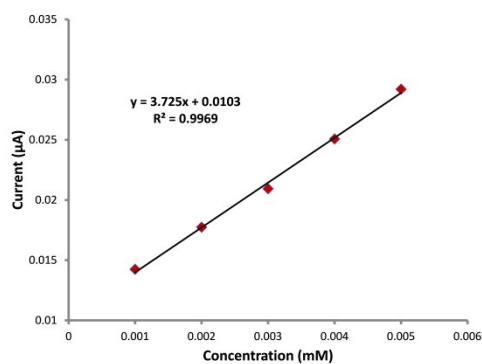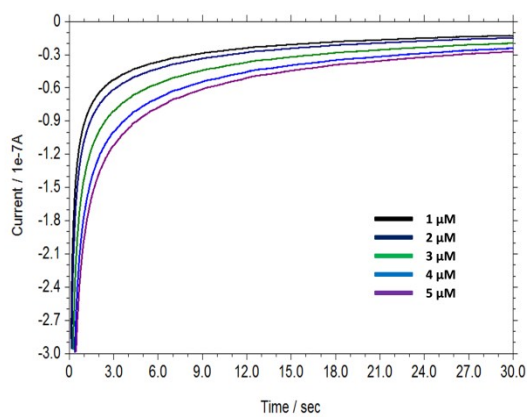
(a)   (b)

Figure S8. (a) Chronoamperograms with increasing concentration of glucose (1.0 µM to 5.0 µM) in 0.1 M PBS (pH 7.0) at [VO(acac)$_2$]-4-PATP-Au electrode at + 0.65 V *versus* Ag/AgCl. **(b)** Plot of concentration of glucose *versus* oxidation peak current. Detection limit 0.1 µM (S/N = 3).


(a)   (b)

Figure S9. (a) Chronoamperograms with increasing concentration of H$_2$O$_2$ (20 to 40 µM) in 0.1 M PBS (pH 7.0) at [VO(acac)$_2$]-4-PATP-Au electrode at - 0.11 V *versus* Ag/AgCl. **(b)** Plot of concentration of H$_2$O$_2$ *versus* reduction peak current. Detection limit 0.03 µM (S/N = 3).

Detection limit of glucose and H$_2$O$_2$ were obtained by using 3σ/m where σ is the standard deviation of peak current in blank solution (n = 25) and m is the slope of the calibration curve.

The S/N value was calculated by dividing the mean value of the currents by the standard deviation of the currents at low concentration of analyte in chronoamperometry.
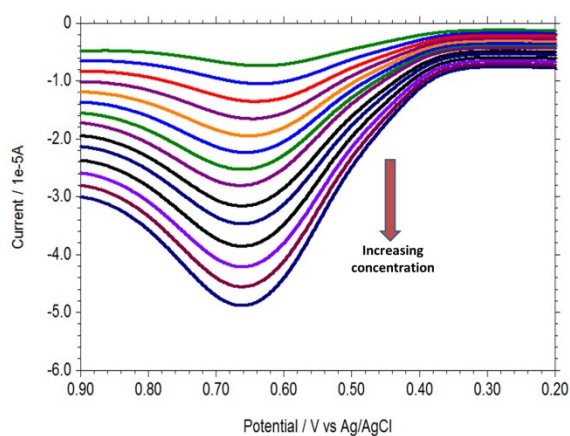
<center>(a)</center>
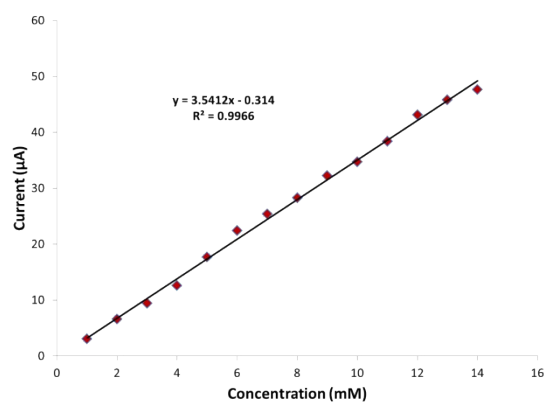
<center>(b)</center>

Figure S10. (a) Overlaid Differential pulse voltammogram with increasing glucose concentration (1-14 mM) in 0.1 M PBS (pH = 7.0) at [VO(acac)$_2$]-PATP-Au electrode **(b)** Plot of current as a function of concentration of glucose with linear trend line (R^2 > 0.99)
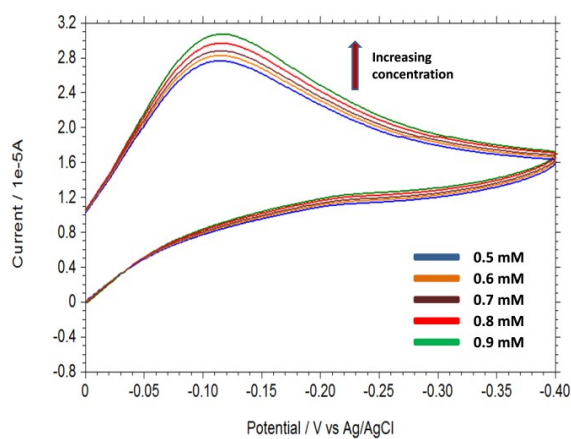
<center>(a)</center>
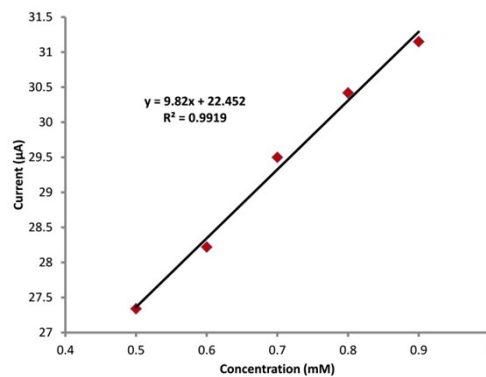
<center>(b)</center>

Figure S11. (a) Overlaid Cyclic voltammograms with increasing hydrogen peroxide concentration in 0.1 M PBS (pH = 7.0) at [VO(acac)$_2$]-PATP-Au electrode **(b)** Plot of current as a function of concentration of hydrogen peroxide with linear trend line (R^2 > 0.99)
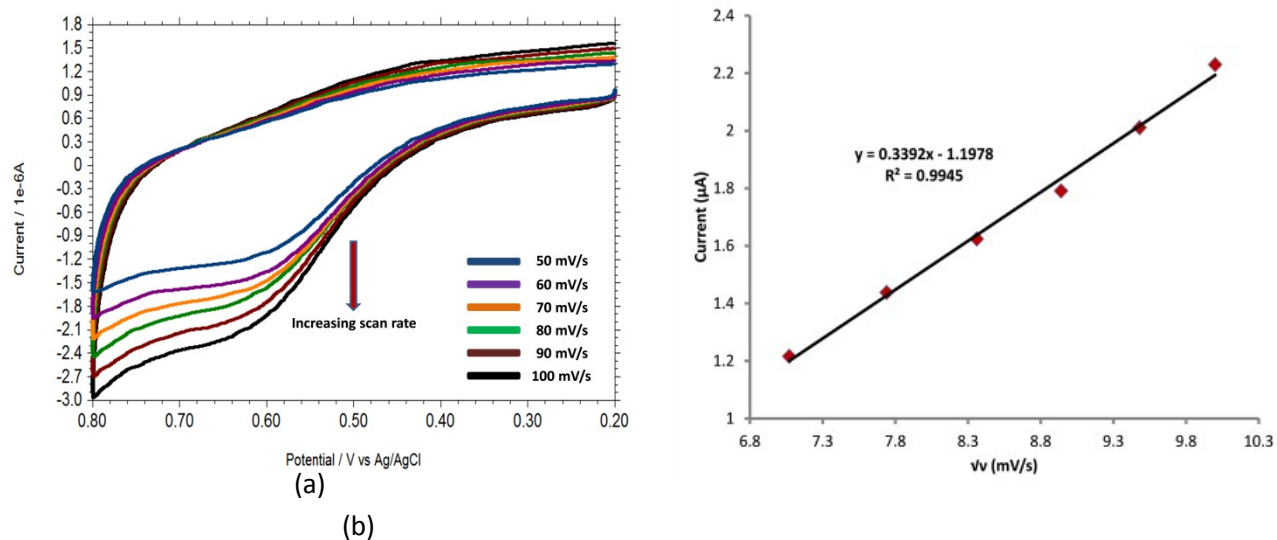
Figure S12. (a) Cyclic voltammograms of 0.1 mM glucose in 0.1 M PBS (pH 7.0) at different scan rate using [VO(acac)$_2$]-PATP-Au electrode (b) Plot of oxidation peak current *versus* square root of scan rate.
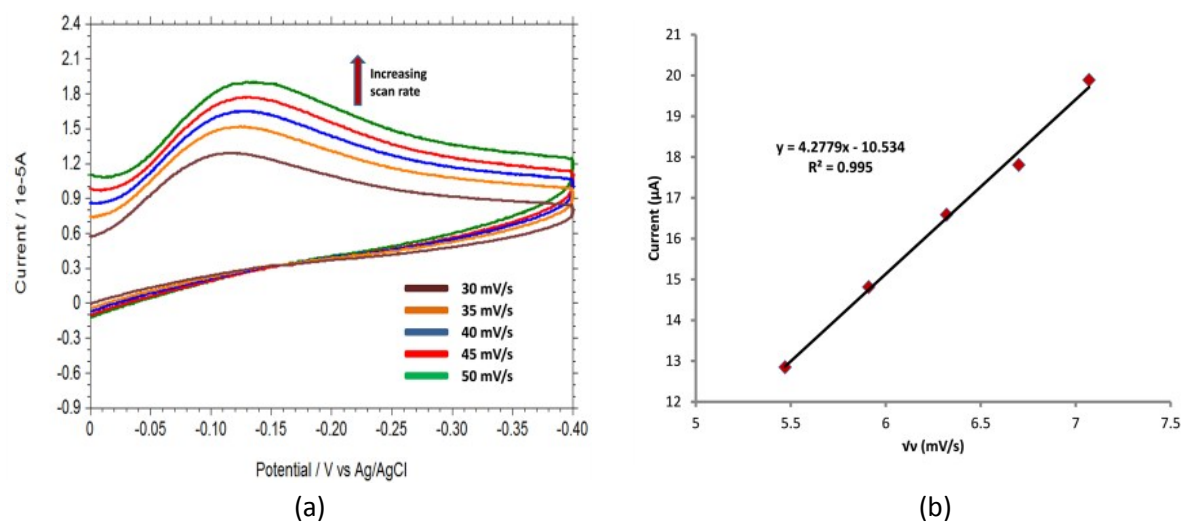
Figure S13. (a) Cyclic voltammograms of 0.5 mM H$_2$O$_2$ in 0.1 M PBS (pH 7.0) at different scan rate using [VO(acac)$_2$]-PATP-Au electrode (b) Plot of oxidation peak current of 0.5 mM H$_2$O$_2$ *versus* square root of scan rate.
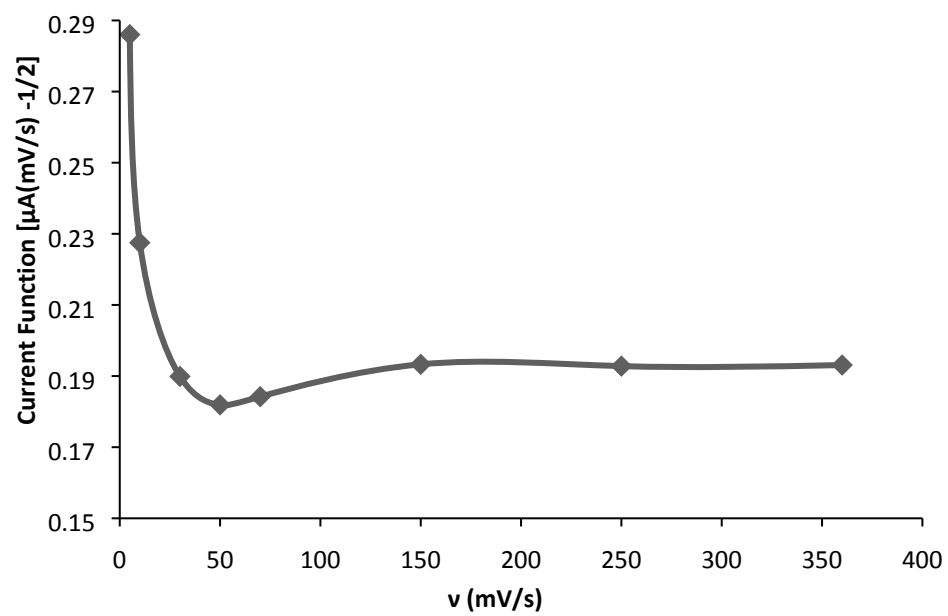
Figure S14. Plot of scan rate –normalized current ($I_p/v^{1/2}$) with scan rate (v)
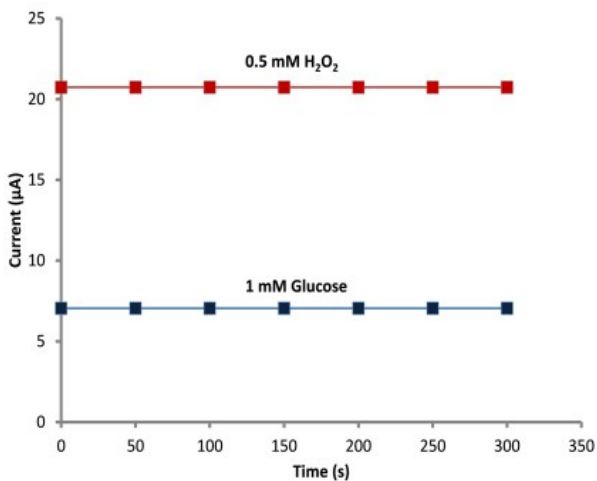
Figure S15. Plot of accumulation time *versus* oxidation peak current of glucose and reduction peak current of H$_2$O$_2$ in 0.1 M PBS at pH 7 at [VO(acac)$_2$]-PATP-Au electrode.
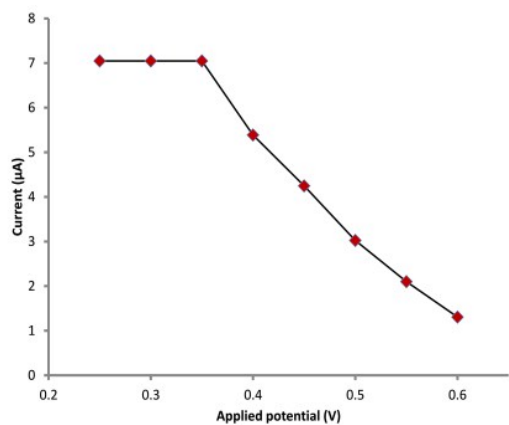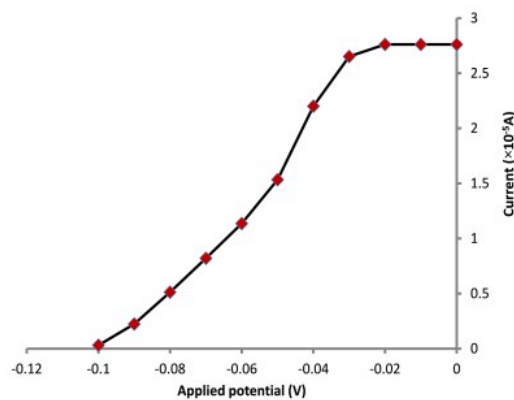
(a)   (b)

Figure 16. (a) Plot of applied potential *versus* oxidation peak current of 0.1 mM glucose in 0.1 M PBS (pH 7) at VO(acac)$_2$-PATP-Au electrode. **(b)**Plot of applied potential *versus* reduction peak current of 0.5 mM H$_2$O$_2$ in 0.1 M PBS (pH 7) at VO(acac)$_2$-PATP-Au electrode.
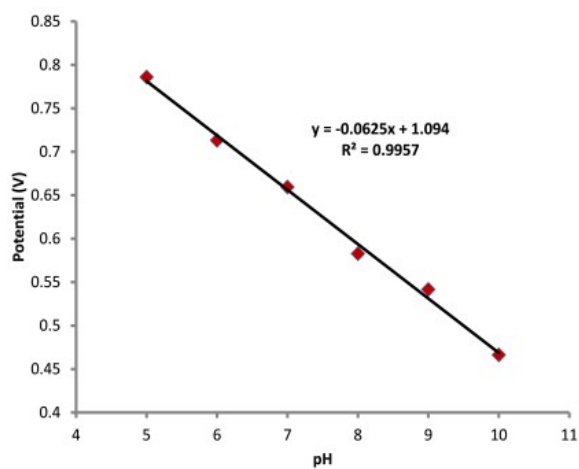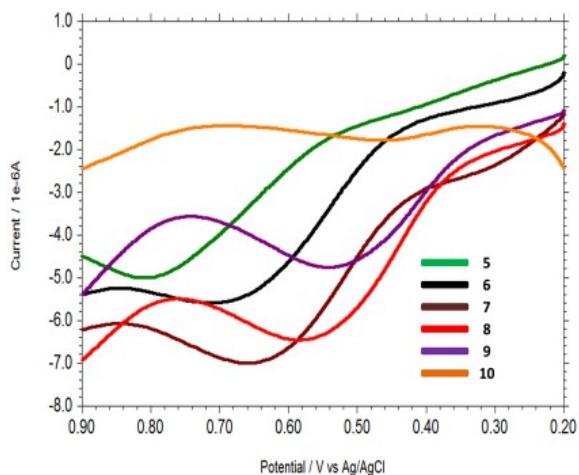
(a)   (b)

Figure S17. (a) Overlaid DPV of 0.1 mM glucose at different pH using [VO(acac)$_2$]-PATP-Au electrode **(b)** Plot of oxidation peak potential of 0.1 mM glucose *versus* pH.
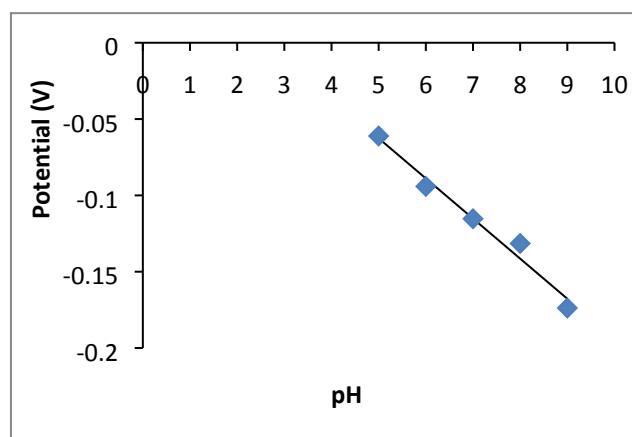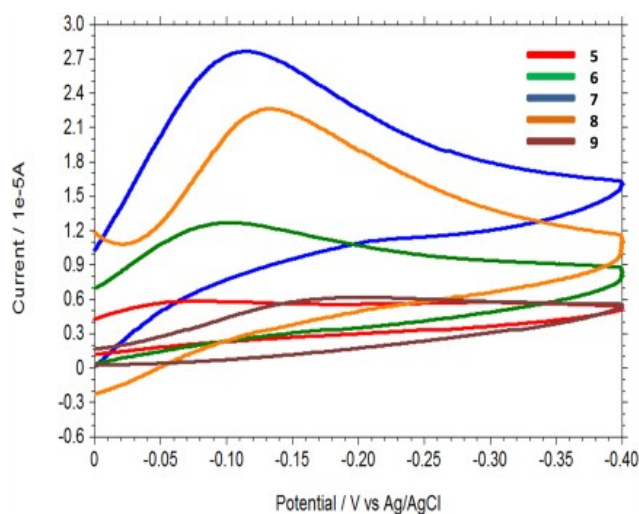
(a)   (b)

Figure S18. (a) Overlaid CV of 0.5 mM H$_2$O$_2$ at different pH obtained with [VO(acac)$_2$]-PATP-Au electrode in 0.1 M PBS. **(b)** Plot of reduction peak current of 0.5 mM H$_2$O$_2$ *versus* pH.
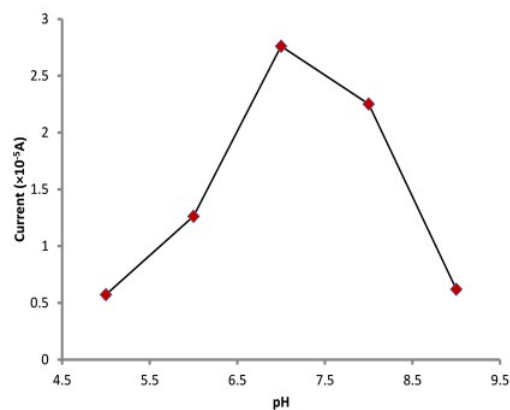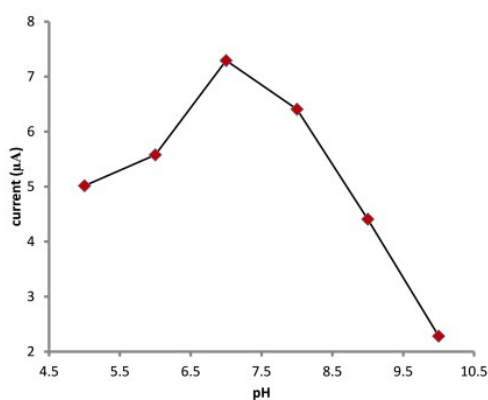
(a)   (b)

Figure S19. (a) Plot of oxidation peak current of 0.1 mM glucose *versus* pH at [VO(acac)$_2$]-PATP-Au electrode in 0.1 M PBS. **(b)** Plot of reduction peak potential of 0.5 mM H$_2$O$_2$ *versus* pH at [VO(acac)$_2$]-PATP-Au electrode in 0.1 M PBS.
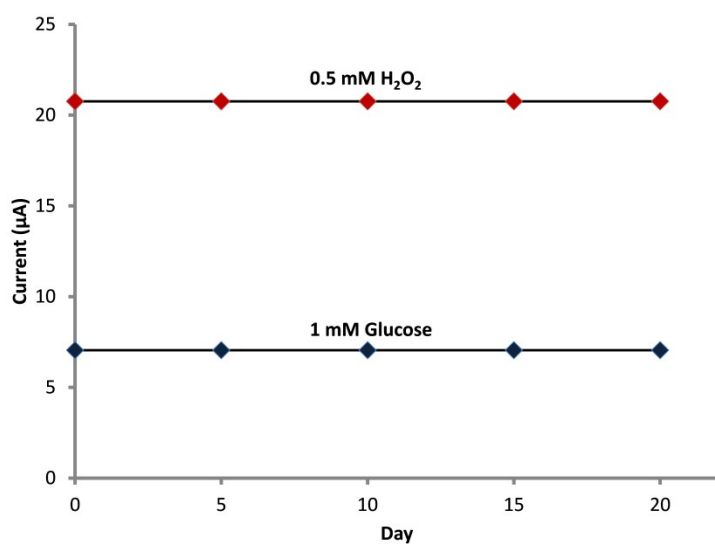
Figure S20. Plot of electrocatalytic current obtained for glucose and hydrogen peroxide with time using [VO(acac)$_2$]-PATP-Au electrode.
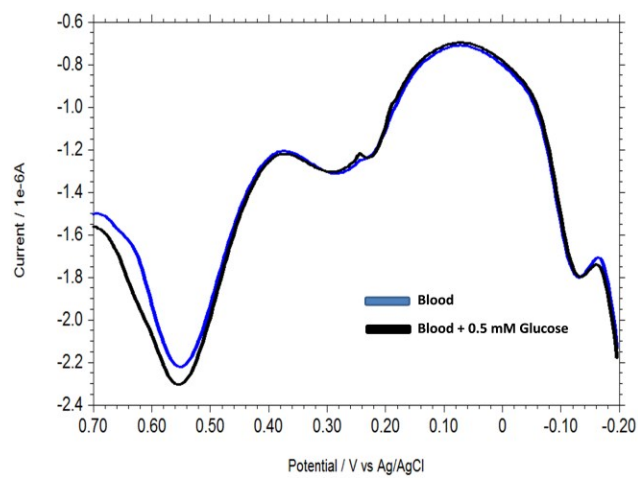
Figure S21. Overlaid DPVs of human blood sample solution and after addition of standard glucose solution in blood sample solution.

Table S1. Comparative account of different non-enzymatic electrochemical sensors for the determination of glucose and hydrogen peroxide

Sensor	Glucose	Hydrogen peroxide

	Linear range (mM)	Detection limit (µM)	Applied voltage (V, *versus* Ag/AgCl)	Medium	Linear range (mM)	Detection limit (µM)	Applied voltage (V, *versus* Ag/AgCl)	Medium	Reference
Cu@M-Chit-CNT/GCE	0.0005-1 .0	0.05	+ 0.5	0.05 M NaOH	0.0001-1.0	0.025	- 0.25	PBS (pH 7.0)	1
Cu_2O/GNs/GCE	0.3 – 3.3	3.3	+ 0.60	0.1 M KOH	0.3-7.8	20.8	-0.4	0.1 M PBS (pH 7.4)	2
CQDs/O_h Cu_2O/Nafion/GCE	0.02-4.3	8.4	+ 0.60	0.1 M NaOH	0.005-5.3	2.8	-0.2	0.1 M PBS (pH 7.4)	3
Mn_3O_4/3DG	0.1 – 8	10	+0.4 0	0.1 M NaOH					4
Au nanocoral/Au	0.05 – 30.0	10	+0.2	0.1M PBS (pH 7.4)					5
Au NW	1– 8	0.05	-0.16	PBS (pH 9.2)					6
CoPcTs/PNPGC	0.25 – 20	100	-	0.1 M NaOH					7
Ni(II)-Curcumin/GC	0.001 - 10	0.1	+0.35	0.1 M NaOH					8
poly[NiTRP]/GCE	0.0025-1.0	360	+ 0.47	1M NaOH					9
CuHCF-AuNP/graphite wax	0.0086-1.2	0.13	+ 0.59	0.1 M KOH					10
Chitosan/AgNPs-G nano composite/GCE					0.1 - 10	7 .0	-0.3	0.2 M PBS (pH 7.4)	11
Ag-MnOOH-GO/GCE					0.0005 - 17.8	0.2	-0.2	0.1 M PBS (pH 7.2)	12
CuO-SiNWs/GCE					0.01-13.18	1.6	-0.3	PBS (pH 7.0)	13
CoOOH nanosheet/Co foil/Au					0-1.6	40	+ 0.1	0.1M NaOH	14
Fe(III)-MPBA-nanoporous gold/Au					0.0009 – 0.5	0.001	-		15
DNA-Cu(II)/GCE					0.0008 – 4.5	0.25	-0.25		16
[VO(acac)$_2$]-PATP/Au	0.1-0.5	0.1	+0.65	0.1 M PBS (pH 7.0)	0.5 – 0.9	0.03	- 0.11	0.1 M PBS (pH 7.0)	Present work

Cu@M-Chit-CNT: Cu nanoparticles decorate on the modified chitosan–CNT; Cu_2O/GNs: Cu_2O nanocubes wrapped by graphene nanosheets); CQDs/O_h Cu_2O: carbon quantum dots (CQDs)/octahedral cuprous oxide(Cu_2O) nanocomposites; 3DG: Three dimensional graphene; Au NW: gold nanowire array electrode; CoPcTs (cobalt (II) phthalocyanine tetrasulfonate); PNPGC: polypyrrole nanofiber onto pencil graphite electrode; poly[NiTRP]: polymeric tetraruthenated nickel porphyrin films; CuHCF: Cu hexacyano ferrate; MPBA: 4-mercapto-3-(phosphonomethylamino) butanoic acid, AgNPs-G: Ag nanoparticles-graphene; Ag-MnOOH-GO: Silver nanoparticle- manganese oxyhydroxide- graphene oxide; SiNWs: silicon nanowires.

Table S2. Determination of glucose in blood sample and H_2O_2 in processed milk with [VO(acac)$_2$]-4-PATP modified gold electrode

Analyte	Sample	Detected	Spiked	Found	RSD[a]	Recovery

					(%)	(%)
Glucose	Blood	5.01 mM	0.5 mM	0.51 mM	2.24	100.2
H_2O_2	Milk	0.91 μM	1 μM	1.01 μM	2.16	101.0

[a] Five times measurements were taken

References

1. Ensafi, A. A.; M. Jafari-Asl, N. Dorostkar, M. Ghiaci, M. Victoria Mart´ınez-Huerta and J. L. G. Fierro, The fabrication and characterization of Cu-nanoparticle immobilization on a hybrid chitosan derivative-carbon support as a novel electrochemical sensor: application for the sensitive enzymeless oxidation of glucose and reduction of hydrogen peroxide. *J. Mater. Chem. B* **2014**, 2, 706 - 717.

2. Liu, M.; Liu, R.; Chen, W. Graphene wrapped Cu_2O nanocubes: non-enzymatic electrochemical sensors for the detection of glucose and hydrogen peroxide with enhanced stability. *Biosens. Bioelectron.* **2013**, 45, 206 - 212.

3. Li, Y.; Zhong, Y.; Zhang, Y.; Weng, W.; Li, S. Carbon quantum dots/octahedral Cu_2O nanocomposites for non-enzymatic glucose and hydrogen peroxide amperometric sensor. *Sensors and Actuators B* **2015**, 206, 735 - 743.

4. Si, P.; Dong, X. C.; Chen, P.; Kim, D. H. A hierarchically structured composite of Mn_3O_4/3D graphene foam for flexible nonenzymatic biosensors. *J Mater Chem B* **2013**, 1, 110–115

5. Cheng, T-M.; Huang, T-K.; Lin, H-K.; Tung, S-P.; Chen, Y-L.; Lee, C-Y.; Chiu, H-T. (110)-Exposed Gold Nanocoral Electrode as Low Onset Potential Selective Glucose Sensor. *ACS Appl. Mater. Interfaces* **2010**, 2, 2773–2780.

6. Cherevko, S.; Chung, C. H. Gold nanowire array electrode for non-enzymatic voltammetric and amperometric glucose detection. *Sens Actuators B* 2009, 142, 216–223.

7. Ozcan, L.; Sahin, Y.; Turk, H. Non-enzymatic glucose biosensor based on overoxidized polypyrrole nanofiber electrode modified with cobalt(II) phthalocyanine tetrasulfonate. *Biosens. Bioelectron.* **2008**, 24, 512 -517.

8. Elahi, M. Y.; Heli, H.; Bathaie, S. Z.; Mousavi, M. F. Electrocatalytic oxidation of glucose at a Ni-curcumin modified glassy carbon electrode. *J. Solid State Electrochem.* **2007**, 11, 273 - 282.

9. Quintino, M. d. S. M.; Winnischofer, H.; Nakamura, M.; Araki, K.; Toma, H. E.; Angnes, L. Amperometric sensor for glucose based on electrochemically polymerized tetraruthenated nickel-porphyrin. *Anal. Chim. Acta* **2005**, 539, 215 - 222.

10. Sivasankari, G.; Priya, C.; Narayanan, S. S. Non-enzymatic amperometric glucose biosensor based on copper hexacyanoferrate-film modified- GNP-graphite composite electrode. *Int. J. Pharm. Bio. Sci.*, **2012**, 2, 188 - 195.

11. Zhang, Y.; Liu, S.; Wang, L.; Qin, X.; Tian, J.; Lu, W.; Chang, G.; Sun, X. One-pot green synthesis of Ag nanoparticles-graphene nanocomposites and their applications in SERS, H_2O_2, and glucose sensing. *RSC Advances*, **2012**, 2, 538 - 545.

12. Bai, W.; Nie, F.; Zheng, J.; Sheng, Q. Novel Silver Nanoparticle–Manganese Oxyhydroxide–Graphene Oxide Nanocomposite Prepared by Modified Silver Mirror Reaction and Its Application for Electrochemical Sensing. *ACS Appl. Mater. Interfaces* **2014**, 6, 5439–5449.

13. Huang, J.; Zhu, Y.; Zhong, H.; Yang, X.; Li, C. Dispersed CuO Nanoparticles on a Silicon Nanowire for Improved Performance of Nonenzymatic H_2O_2 Detection. *ACS Appl. Mater. Interfaces* 2014, 6, 7055–7062

14. Lee, K. K.; Loh, P. Y.; Sow, C. H..; Chin, W. S.; CoOOH nanosheet electrodes: Simple fabrication for sensitive electrochemical sensing of hydrogen peroxide and hydrazine. *Biosens. Bioelectron*. **2013**, 39, 255–260.

15. Zheng, M.; Li, P.; Yang, C.; Zhu, H.; Chen, Y.; Tang, Y. W.; Zhou, Y. M.; Lu, T. H. Ferric ion immobilized on three-dimensional nanoporous gold films modified with self-assembled monolayers for electrochemical detection of hydrogen peroxide. *Analyst* 2012, 137, 1182–1189

16. Zeng, X.; Liu, X.; Kong, B.; Wang, Y.; Wei, W. A sensitive nonenzymatic hydrogen peroxide sensor based on DNA–Cu^{2+} complex electrodeposition onto glassy carbon electrode. *Sens Actuators B* **2008**, 133, 381 - 386.